Lignin Carbohydrate Complexes structure preserved throughout downstream processes for their valorization after recovery from industrial process water

Virginie Steinmetz, Maud Villain-Gambier, Armand Klem, Isabelle Ziegler, Stéphane Dumarcay, Dominique Trebouet

j.ijbiomac.2019.11.238.

Lignin Carbohydrate Complexes structure preserved throughout downstream processes for their valorization after recovery from industrial process water

Virginie STEINMETZ[a,b], *Maud VILLAIN-GAMBIER**[a], *Armand KLEM*[c], *Isabelle ZIEGLER*[b], *Stéphane DUMARCAY*[b], *Dominique TREBOUET*[a]

[a] Laboratoire de Reconnaissance et Procédés de Séparation Moléculaire (RePSeM), Université de Strasbourg, Institut Pluridisciplinaire Hubert Curien (IPHC), UMR CNRS 7178, 25 rue Becquerel, 67087 Strasbourg Cedex 2, France

[b] Laboratoire d'Etudes et de Recherche sur le Matériau Bois, EA 4370 USC INRA 1445, Boulevard des Aiguillettes, BP 70239, 54506 Vandoeuvre lès Nancy, France

[c] Norske Skog Golbey, Route Jean-Charles Pellerin, BP 109, 88194 Golbey, France

* Corresponding author email: maud.villain@unistra.fr, tel: +33(0)368852748

KEYWORDS: thermomechanical process, membrane filtration, Lignin-Carbohydrate Complexes (LCCs), thermal treatment, downstream process, structural analysis, py-GC-MS, 2D-NMR.

ABSTRACT: Firstly studied and pointed out because of their major role in wood recalcitrance to delignification, LCCs are gradually raising interest about their own valorization. Their recovery from residual feedstocks of lignocellulosic biomass has been the topic of several recent papers in the field while other studies report about their various interesting properties. Considering their future industrial production, this work is focused on evaluating the impact of different downstream processes (DSP) on their structure including moist heat sterilization, simple effect evaporation and spray-drying. LCCs were recovered from the mill water of a thermomechanical plant by successive membrane filtration steps. Samples were taken after the different DSP and compared to a freeze-dried control. Global and structural characterizations given by elemental analysis, acid hydrolysis, pyrolysis coupled to gas-chromatography, SEC, ^{13}C and 2D-HSQC NMR showed that the LCCs structure is well preserved during all of these DSP. This paper demonstrates the feasibility of producing high quality industrial LCC grade for commercialization in integrated biorefineries.

INTRODUCTION Lignin Carbohydrate Complexes (LCCs) have been attracting increasing attention these recent years in the field of lignocellulosic biorefineries. LCCs are released during the first pretreatment step targeting the deconstruction of the biomass for its individual components valorization. They originate from the fragmentation of hemicelluloses and lignin which are covalently linked under their native state in wood.[1] LCCs were firstly studied in the pulp industry because of their major role in the recalcitrance of wood biomass to delignification.[2,3] A lot of work was done on their characterization to better understand the structures preventing the total separation of wood fibers and also because they act as inhibitors during the enzymatic hemicellulosic sugar hydrolysis for biofuel production.[4–6] Nowadays, their composite nature including aromatic and sugar moieties appears to be an opportunity for new bio-based products development and LCCs tend to be considered as high

added-value coproducts. The production of gas-barrier films through enzymatic LCCs polymerization was reported by Oinonen *et al.* providing a new biomaterial for food packaging with high oxygen barrier property.[7] LCCs amphiphilic structure also confers them surfactant properties and potential applications as drug carriers.[8,9] Their biological properties were as well described in various papers including their antioxidants and anti-UV efficacies for cosmetic development and their pharmacological activities for human medicine.[10–13]

For industrial purposes, it has been demonstrated that LCCs could be recovered from various residual feedstocks of lignocellucosic biomass. Narron *et al.* deciphered their presence in the hydrolyzates resulting from the autohydrolysis pretreatment of hardwood and nonwood biomasses.[6] They successfully achieved their recovery by means of a selective adsorption on a polymeric resin reaching approximately 90 % of soluble lignin recovery. Zhang *et al.* also isolated LCCs from the hydrolyzate of Norway spruce, a softwood specie, using specific resin adsorption followed by gradient dialysis processes.[11] A previous study, on lab-scale extracted LCCs, showed that the combination of precipitation and diafiltration leaded to the development of a universal method for LCCs fractionation and purification disregarding their biomass origin.[14] Westerberg *et al.* also reached a good separation of lignin, hemicelluloses and LCCs from hot-water extracted Norway spruce by combining membrane filtration and adsorption based processes.[15] As depicted by those examples, an increasing interest for LCCs recovery from autohydrolyzates or hot water extraction liquor from biorefineries pretreatments can clearly be noted at this time. Additionally, membrane filtration processes have also been successfully applied for the recovery of LCCs from the liquid effluents of the pulp and paper industry. Al Rudainy *et al.* isolated high molecular weight LCCs from sodium-based spent sulfite liquor using a 50-kDa polysulfone membrane.[16] A final purity of 93% and product yield of 43.4% was achieved following an additional diafiltration. Ultrafiltration of the process water discarded from thermomechanical treatment (TMP) also demonstrated to

lead to an interesting sourcing of LCCs characterized by their well-preserved native structure.[17]

While LCCs potential for industrial applications is most of the time assessed right after their isolation at lab-scale, further downstream processes (DSP) will have to be taken into consideration for preservation and transportation purposes before their incorporation into final industrial products. Such downstream treatments often suggest heat exposure of the product whereas hemicelluloses and lignin structures present poor thermal stability. The main effects of elevated temperatures on hemicelluloses reported in the literature are deacetylation, dehydration, depolymerization, monomer degradation into furfural derivatives and carbonization.[18] Heat-denaturized lignin is characterized by a reduced number of aryl ether linkages, an increased number of condensed (carbon-carbon) interunit bonds and a demethylated and deoxygenated backbone.[19,20] These chemical degradations often start to take place while the temperature reaches 200 to 250 °C in dry processes but also happen at lower temperatures in aqueous media like observed by Giummarella *et al.* during the hydrothermal treatment of softwood for 2h at 160 °C.[4] Such extensive heat-sensitivity underlines the importance of selecting and optimizing appropriate DSP in order to preserve the LCCs structure during their production phase.

In this work, LCCs were recovered from the process water of a TMP plant by successive membrane filtration steps as reported previously.[17] Different DSP were then applied including moist heat sterilization, simple effect evaporation for concentration under reduced pressure and spray-drying. Analytical tools were combined to provide a deep chemical and structural characterization of the LCCs along these processes. The understanding and control of the DSP impact on LCCs structure is important for the research and development of future final products. The general purpose of this paper is to provide new insights on LCCs stability for their valorization and commercialization in integrated biorefineries.

EXPERIMENTAL SECTION

Materials

The TMP process water used for this study came from Norske Skog Golbey industry France. Spruce and fir were used as primary raw materials in the pulp mill. The dissolved LCCs were recovered from 3 m^3 of process water using pilote-scale flotation and filtration units (Figure 1) as previously reported.[17] The LCC rich fraction was recovered after ultra-filtration on the 1 kDa membrane.

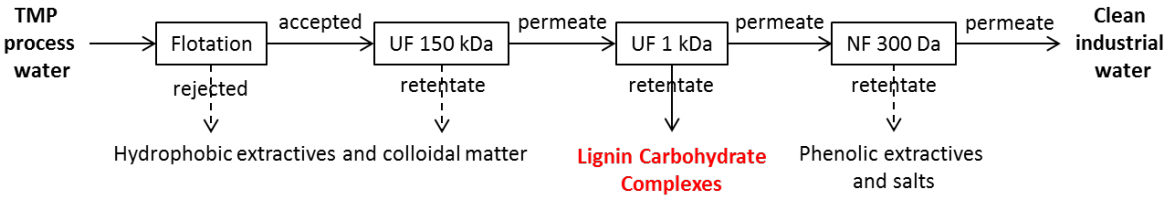

Figure 1. Schematic illustration of the overall process of TMP water treatment and LCCs recovery.

Downstream processes (DSP)

The figure 2 illustrates the different treatments applied to the LCC rich fraction (1 kDa retentate) and the origin of the different samples characterized in this work. Moist heat sterilization was performed as follow: 750 mL of 1 kDa retentate were placed in a glass resistant bottle with semi-closed cap and sterilized for 20 min at 121 °C under pressure. The autoclaved retentate was thus freeze-dried for analysis. Evapo-concentration and spray-drying were performed as follow: the 1 kDa retentate was continuously concentrated under reduced pressure (500 to 700 mbar) on a simple effect evaporator (EVV/1000) from Pignat. The concentration was stopped when the retentate reached a dry matter content of approx. 5 %. Under those conditions the retentate maximum temperature was maintained at around 85-90 °C during all the process. The evapo-concentrated retentate (EC) was then kept at 65 °C for spray-drying on a Büchi B-290 mini spray-dryer. The inert loop was enabled with pressurized air as atomizing gas with a flow rate of 570 $L.h^{-1}$. A 2-fluid nozzle with 0.7mm cap was

employed for atomization. The aspirator was set to 100 % (35m ^{3}.h^{-1}), the inlet temperature to 190 °C and the feed flow to 0.9 L.h^{-1}. A sample of EC was taken prior to spray-drying and freeze-dried for analytical purposes.

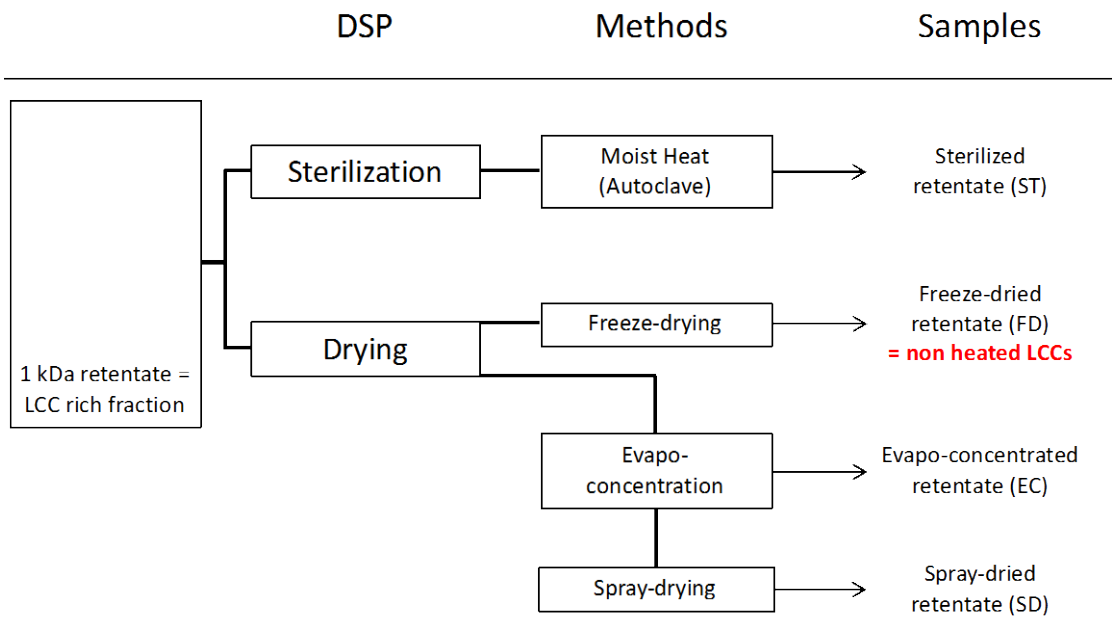

Figure 2. Schematic illustration of the 1 kDa retentate downstream treatments and sampling.

Global composition

The global organic composition of the four samples was determined after acid hydrolysis following the protocol described elsewhere.[17] The experiments were performed in triplicates and results are expressed as mean values with standard deviations. The weight percentages of nitrogen, carbon, hydrogen and oxygen of the freeze-dried and spray-dried samples were determined using an elemental analyser (FLASH 2000 Thermofischer). The analyses were performed in duplicate.

Pyrolysis coupled to Gas chromathography/Mass spectrometry (Py-GC/MS)

Pyrolysis of the four samples (approx. 0.5 mg per quartz tube) were performed with a CDS 5150 Pyroprobe connected to a Clarus 580 GC system equipped with a DB-5MS capillary column (Agilent J&W, 30 m x 250 µm i.d., 0.25 µm film thickness) and a Clarus 500 mass detector (EI+ at 70 eV). The pyrolysis was performed at 650 °C during 15 s. After pyrolysis,

the products were flushed into the GC with helium as a carrier gas at 1 $mL.min^{-1}$. The temperature profile of the GC for products separation was as follow: the GC column was initially maintained at 50 °C for 5 min, then ramped up to 280 °C at a rate of 5 $°C.min^{-1}$, and finally held at 280 °C for 9 min. The compounds were identified using the NIST 2011 mass spectral library and the literature.[11,21,22] The pyrograms were integrated by regions corresponding to the carbohydrate, lignin and extractive pyrolytic products. Wood sawdust and MWL prepared from the same wood feedstock as NSG were used as standard to define the different regions. The total ion current (TIC) areas of each region were expressed as relative percentages by normalizing the sum of the integrated areas to 100 %. The lignin derivative regions were further treated by individually integrating the identified phenolic peaks to determine the lignin thermal fragmentation patterns and G/H ratios of each sample. The experiments were performed in triplicates and results are expressed as mean values with standard deviations.

NMR experiments

For all NMR analyses about 100 mg of samples were dissolved in 0.5 mL of DMSO-d6. Spectra were recorded on a Bruker AVANCE III 300 MHz spectrometer equipped with a BBO probe 5 mm at 25 °C. For quantitative ^{13}C NMR, an inverse gated decoupling sequence was used with a relaxation delay of 12 s and 13K scans were acquired. 2D-HSQC NMR spectra were acquired with the following parameters: 128 transients, 16 dummy scans, relaxation delay of 1.9 s, 1024 data points in F2 (1H) dimension and 256 data points in F1 (13C). A coupling constant $1J_{C-H}$ of 145 Hz was used. The 2D data set was processed with MestreNova using a 90° shifted square sine-bell apodization window. The data matrices were zero filled to 1024 points in both dimensions, baseline and phase corrections were applied in both dimensions. The central solvent (DMSO) peak was used as an internal chemical shift reference point (δ_C/δ_H 40.4/2.51).

Size Exclusion Chromatography (SEC)

The molar mass distribution of the lignin was determined using an aqueous SEC method on a Prominent Shimadzu HPLC equipped with a guard column Phenomenex Polysep GFC-P (7.8 x 35 mm) and two analytical columns Phenomenex Polysep P4000 (7.8 x 300 mm) and P3000 (7.8 x 300 mm). The chromatographic conditions and sample preparation used were as previously reported.[17] Measurements were carried out in triplicate.

RESULTS AND DISCUSSION

DSP choice and optimization. In this study, the freeze-dried retentate (FD) represents the non-degraded or denaturized LCCs sample as this DSP does not require heat exposure. Its complete analytical characterization has already been published.[17] The others downstream processes were selected among various industrial options based on their cost and environmental impact for their integration in biorefineries as mentioned thereafter.

Due to their high sugar content, LCCs are particularly sensitive to microbial contamination and need to be well preserved if kept as aqueous solution. While the 1 kDa retentate was concentrated until a volume reduction of 21 by ultrafiltration, the limit of LCCs water solubility was outreached resulting in the production of a stable suspension. No further sterile filtration was thus possible and heat moist sterilization was applied as a physical preservative treatment to limit the use of chemical preservatives. Even if this DSP can be easily avoided at industrial scale by working under aseptic conditions, it was considered interesting to present these results as they give complementary information about the resistance of LCCs to heat exposure under pressure.

For long term storage, stability and cost-effective transportation, dehydration or drying processes are preferred at industrial scale for the preservation of natural products such as food or biomass derivatives.[23] Freeze-drying was excluded from the industrial drying process

options as this technique is too expensive while considering its integration in biorefineries due to its high energetic consumption and extended process time in batch mode. In comparison, spray-drying is a continuous and fast process presenting various advantageous such as a short heat exposure of the products and a good control of the final particles characteristics.[24] In the end, the spray-dried products present facilitated handling and formulation. To reduce the cost of the drying process, a previous dehydration step was conducted by evapo-concentration. This process is economic as it is low energy consuming and allows the recycling of the evaporated water. Evaporation can be performed under reduced pressure decreasing the water boiling point and thus the process temperature and LCCs degradation. The use of evapo-concentration followed by spray-drying allowed the production of a fine powder presented in picture 1. The overall process was optimized along different batches. The 1kDa retentate was concentrated from 2.5 to 5 % of dry weight by evapo-concentration. The maximum EC concentration was set at 5 % as aggregation phenomena were observed while reaching higher concentrations. The viscosity of the EC was reduced from 20 $mPa.s^{-1}$ (at 20 °C) to 8 $mPa.s^{-1}$ by maintaining its temperature at 65°C prior to atomization. This condition was mandatory to ensure a good feeding rate and avoid nozzle clogging.

Picture 1. Final powder obtained after evapo-concentration and spray-drying of the 1 kDa retentate.

Global composition. The chemical compositions of the four samples are given in Table 1 and expressed as relative percentages of the dry matter. All samples present almost exactly the same dry weight composition with carbohydrates accounting for approx. 57 %, lignin and ashes together for 27 % and non-characterized matter, regrouped under "others" name, reaching around 15 %. Considering the relative abundance of sugars monomers, mannose units represent 61 to 62 % of the total polysaccharides content in the different samples followed by glucose and galactose units representing 19 to 20 and 13 to 14 % respectively. These results indicate that there is no change in the global composition of the LCC rich fraction at a molecular level regardless of the DSP applied. The carbohydrate moiety of LCCs is well preserved and composed of galactoglucomannans (GGM) with a Man:Glc:Gal ratio of 3:1:0.6.

Table 1. LCCs rich fraction global composition after different DSP: FD-freeze-dried; EC-evapo-concentrated; SD-spray-dried; ST-sterilized; AIR-Acid insoluble residue including ashes; ASL-acid soluble lignin. Values are given as mean of triplicates and standard deviations indicated in brackets.

	Dry wt%	**FD**	**EC**	**SD**	**ST**
Sugars	Fuc	nd	nd	nd	nd
	Rha	0.06 (0.04)	0.06 (0.05)	0.06 (0.00)	0.05 (0.02)
	Ara	1.07 (0.07)	0.98 (0.14)	1.16 (0.07)	0.99 (0.07)
	Gal	7.20 (0.50)	7.74 (0.87)	7.43 (0.18)	7.38 (0.40)
	Glc	11.64 (0.66)	10.93 (0.04)	11.88 (0.13)	11.05 (0.56)
	Xyl	0.38 (0.04)	0.37 (0.05)	0.46 (0.02)	0.34 (0.06)
	Man	34.67 (0.96)	34.38 (1.53)	36.14 (0.24)	34.79 (1.70)
	GalA	1.68 (0.51)	2.03 (0.42)	1.35 (0.06)	1.34 (0.10)
	GlcA	0.28 (0.10)	0.26 (0.05)	0.21 (0.00)	0.26 (0.04)
	Sum	57.0 (2.9)	56.8 (3.1)	58.7 (0.7)	56.2 (3.0)
Aromatics	AIR	23.1 (0.1)	19.9 (0.3)	18.2 (0.6)	21.3 (0.6)
	ASL	7.3 (0.2)	6.4 (0.4)	8.5 (0.2)	6.9 (0.2)
	Sum	30.4 (0.3)	26.3 (0.7)	26.7 (0.8)	28.2 (0.8)
Others		12.6 (3.2)	16.9 (3.8)	14.6 (1.5)	15.6 (3.8)

Table 2. Elemental analyses of the control LCC rich fraction (FD) and the fraction after evapo-concentration and spray-drying (SD).

	N %	C%		H%		O%
FD	<0,3	47,89	(3,52)	6,07	(0,41)	46,04
SD	<0,3	47,88	(0,06)	6,18	(0,06)	45.94

The elemental compositions of the freeze-dried and spray-dried samples are presented in Table 2. Their comparison shows that the elemental distribution of the LCC rich fraction is also preserved during the concentration and drying processes. It is interesting to note that the data generated for the spray-dried sample (both in global and elemental analyses) are highly reproducible compared to the other samples. This fact is probably explained by the fineness and homogeneity of the powder produced by this process. The oxygen content being stable throughout the processes, the functionalization of LCCs in the fraction is supposedly not affected by the process as well. Indeed, if occurring, thermal degradation reactions such as sugar dehydration or lignin condensation would have led to an oxygen content decrease. This observation supports the previous results in indicating that the DSP used in this work are efficiently preserving the LCCs. To consolidate this information, the evolution of the most thermal sensitive structures in LCCs, i.e. glycosidic bonds and acetyl groups in hemicelluloses, ether linkages in lignin and phenyl glycoside bonds, was monitored by chromatographic and spectroscopic methods.[4]

Size exclusion chromatography. The apparent molecular weight (aMW) of LCCs in the four samples was monitored by SEC as featured in Figure 3. Any polymerization or depolymerization reactions occurring during the DSP would be detected by this method and result in an evolution of the molecular weight distribution of the samples. As can be seen at 280 nm and with the RID detector, the chromatograms of the four samples present the same molecular weight distributions. A really slight and progressive shift of the chromatograms to

the right is observable but attributed to the employed method (progressive clogging of the column). The differences observed in intensity result from the variation during sample weighting. The LCCs of all samples are characterized by an apparent molecular weight ranging from 4 to 9 kDa. This result indicates the no polymerization or depolymerisation reactions were driven by the different DSP. Analytical pyrolysis and NMR experiments have been conducted to evaluate other possible internal rearrangements or small structural losses.

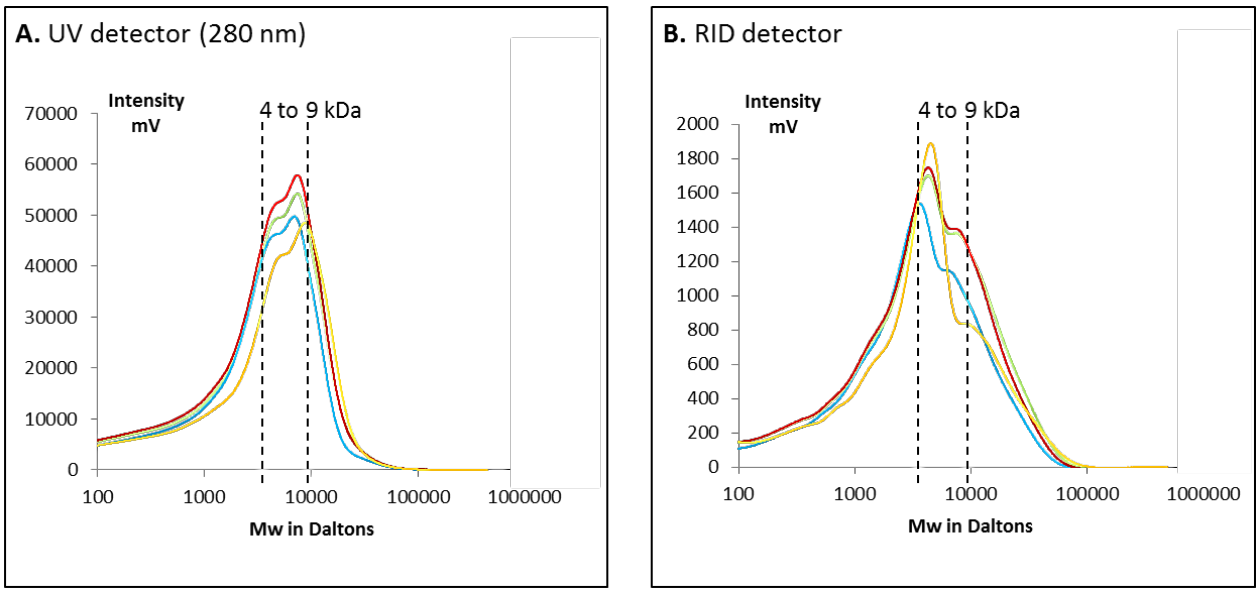

Figure 3. SEC chromatograms of the four sample with (A) UV and (B) RID detectors: FD in blue; EC in orange; SD in green and ST in red.

Pyrolysis experiments. The total pyrograms of the four samples are shown in Fig. 4. All the identified peaks with their retention time are listed in supporting information (Table S1). Carbohydrate pyrolytic products, including numerous furfural derivatives, are mainly encountered at the beginning of the pyrograms from 3 to 13 min. In addition, the 5-hydroxymethylfurfural (HMF) elutes at around 19.1 min for all samples while the typical anhydrosugars formed during pyrolysis of polysaccharides appear as broad and overlapping peaks in the range of 25 to 30 min. Phenolic pyrolytic products are mainly concentrated in the

region from 10 to 32 min, sometimes interspersed by carbohydrate signals. The presence of extractives in all samples is pointed out at the end of the pyrogams with signals identified as saturated fatty acids, terpenes and lignans. The identification of these constituents completes the previous global analysis giving a deeper understanding of the "other" category composition. It is worth noting that these extractives remain in the different fractions despite the flotation and membrane filtration processes and regardless to the DSP applied. The persistence of fatty acids in technical lignins, even after organosolv and alkaline pretreatments, has also been observed by Constant *et al.*[25]

Among the carbohydrate signals of all samples, characteristic products from the pyrolysis of hexose containing hemicelluloses have been identified such as furfural, furfuryl alcohol, 2-(5H)-furanone and 5-methylfurfural as well as an important signal corresponding to HMF. The production of HMF along pyrolysis of hemicelluloses has indeed been reported by Werner *et al.* with the highest amounts associated to galacto and glucomannans pyrolysis.[26] These observations are consistent with the monomeric sugar analyses of the samples.

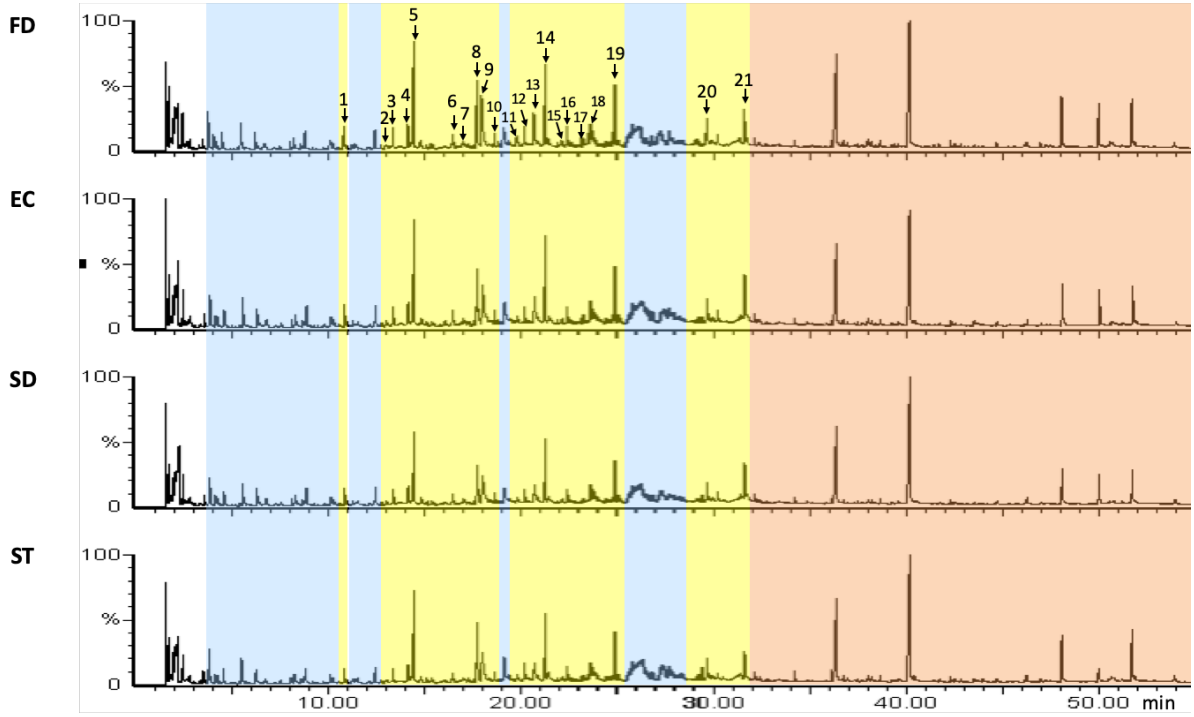

Figure 4. Pyrograms of the four LCC rich samples after different DSP. The integrated regions accounting for (a) carbohydrate derived signals are indicated in bleu, (b) lignin derived signals in yellow and (c) extractives derived signals in orange. Numbers indicate the identified peaks integrated in Fig. 5.

Table 3. Relative abundances of carbohydrate, lignin and extractive derivatives arising from the py-GC/MS analyses of the four LCC rich samples.

	FD	EC	SD	ST
Carbohydrate derivatives				
total	34,3 (1,9)	36,0 (1,7)	36,6 (1,8)	37,7 (0,2)
Lignin derivatives				
total	45,7 (0,9)	44,1 (1,8)	44,7 (3,0)	42,8 (1,0)
G/H ratio	91:9	90:10	90:10	90:10
Extractives				
total	20,0 (1,0)	20,0 (3,4)	21,0 (2,4)	19,5 (1,1)
fatty acid	14,2 (1,6)	15,2 (3,6)	15,7 (2,8)	14,1 (1,8)
others	5,7 (0,6)	4,8 (0,2)	5,3 (0,3)	5,4 (1,4)

The relative abundances of carbohydrate, lignin and extractive pyrolytic products are reported in Table 3. The relative distributions of the four samples are identical with around 36 % of the signal associated to carbohydrates, 44 % to lignin and 20 % to extractives. This distribution is different from the one obtained by acid hydrolysis of the samples (Table 1). The high pyrolytic temperature, which is higher to the carbonization temperature of hemicelluloses, explains that carbohydrates are underestimated in pyrolytic analyses compared to other widespread chemical methods.[18] However, there is still a good correlation between the pyrolysis and chemical results as both methods show a stable composition of the fraction throughout all the different DSP. The development of a standardized py-GC/MS protocol for the global analysis of lignocellulosic biomass could be an interesting fast, easy-handling and economic alternative to current chemical methods.

Meanwhile, py-GC/MS is already a useful tool for lignin structure analysis.[21,25,27,28] As can be seen in Table 3, there is no noticeable change in the G/H ratio of the four samples regardless of the DSP. In Figure 5, around 20 phenolic components identified in the lignin region were integrated as individual peaks and expressed as relative area percentages of the total aromatic region. The lignin thermal fragmentation pattern observed is identical for the four samples compared. For all samples, the major aromatic components identified are catechol > guaiacol > p-vinylguaiacol > p-methylguaiacol ≈ p-methylcatechol ≈ coniferaldehyde. As no ferulic acids enter in the composition of the LCC rich fraction (2D NMR spectra in Figure S1), the high amount of p-vinylguaiacol in this work solely arises from lignin degradation. The high amount of C-type components (catechol derivatives) can be explained by the high pyrolysis temperature of 650 °C responsible of guaiacol demethylation, particularly occurring at temperature ranging from 600 to 700 °C .[21] In this sense, the major aromatic components constituting the lignin present in the four samples are: guaiacol representing around 31 % of the total phenolic signal (as the sum of guaiacol and catechol

relative abundances), p-methylguaiacol accounting for ca. 17 % (p-methylguaiacol and p-methylcatechol) and p-vinylguaiacol yielding around 10 %. This composition tends to indicate a high aryl ether content in the samples as guaiacol has been reported as a pyrolytic product directly arising from β-O-4 cleavage.[21]

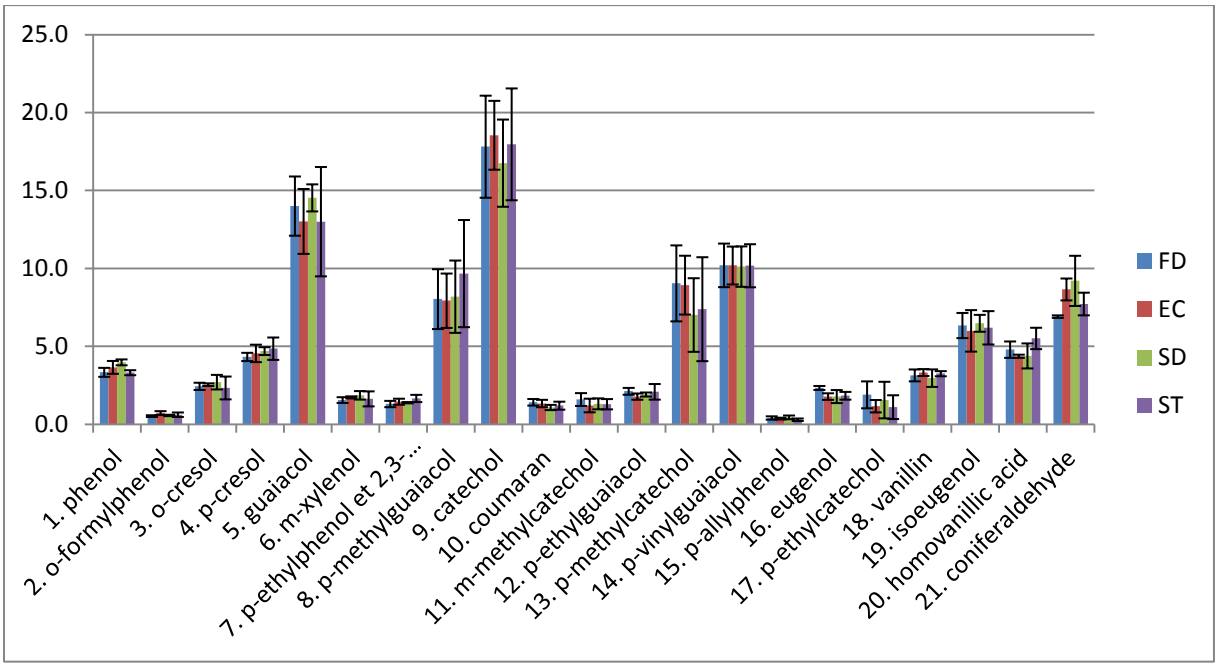

Figure 5. Relative distribution of the phenolic pyrolytic products of the four samples expressed as percentages of the total aromatic region area.

NMR experiments. The 2D-HSQC NMR was employed to identify and compare the lignin carbohydrate and lignin interunit linkages (LCLs and LILs respectively) composing the LCCs of the four samples. The structures depicted through this method are presented in Figure 6. Assignments of the cross peak signals were made according to reputable publications (Table S2).[4,25,29,30] Quantitative ^{13}C NMR was combined to 2D-HSQC study for the quantification of the different linkages giving further information on the lignin condensation state. The acetylation pattern of the hemicellulosic moiety in LCCs was also studied through these technics as deacetylation has been reported during thermal treatment of hemicelluloses.[4,31]

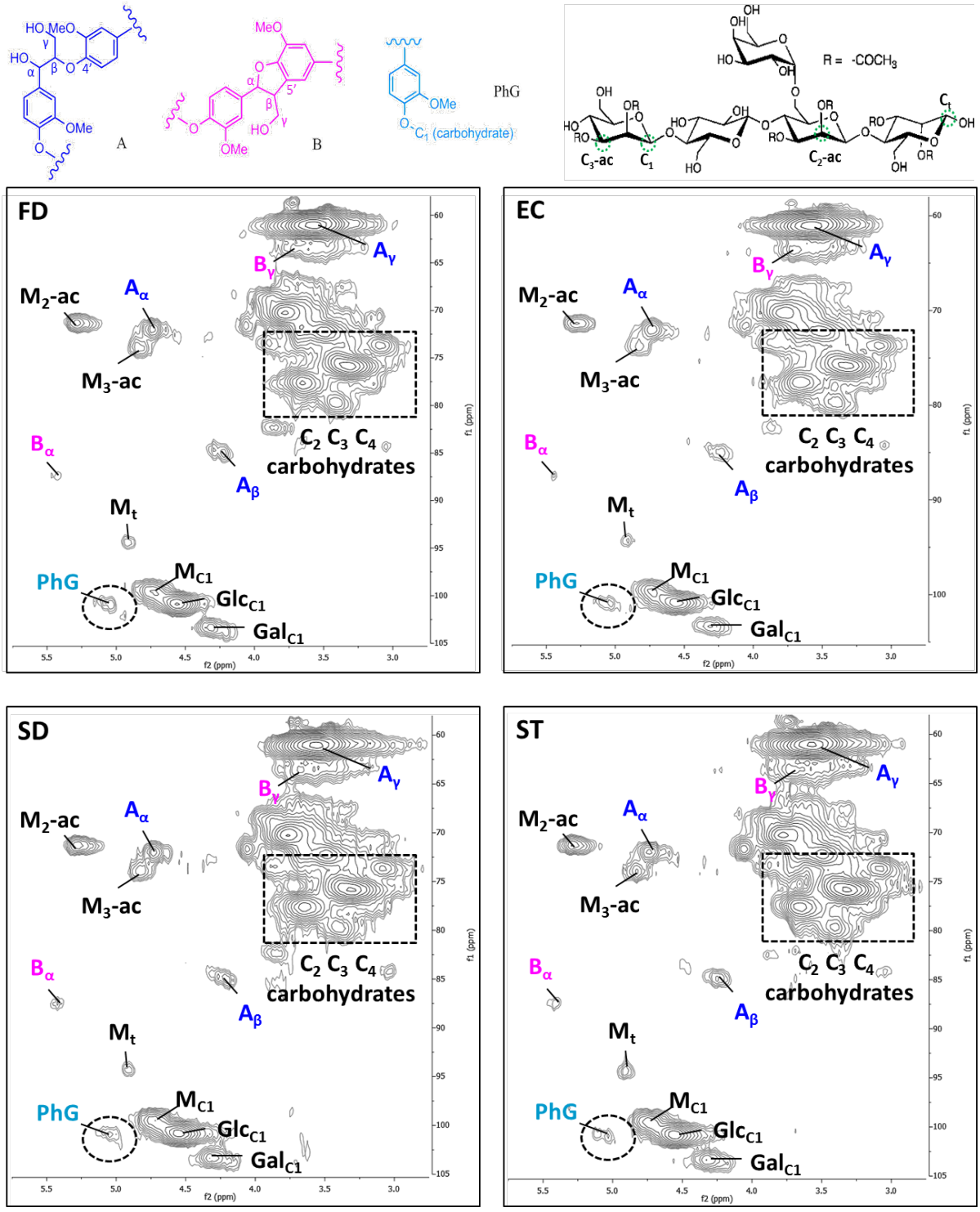

Figure 6. Main structures identified and quantified by NMR spectroscopy: (A) β-O-4’ aryl ether; (B) β-5’ phenylcoumaran; (PhG) phenyl glycoside linkages and 2D-HSQC aliphatic regions of the four samples: M=mannose, Glc=glucose and Gal=galactose, t subscript indicates the terminal reducing end, -ac subscript stands for acetylated carbon.

The aromatic regions of the 2D-HSQC NMR spectra of all samples (δ_C/δ_H 105-155/6-8) are only composed of G unit signals, in line with the absence of syringol derivatives in the pyrolytic products and as expected for softwood lignin (Figure S1). The aliphatic regions of all spectra (δ_C/δ_H 50-105/2.5-6.5) are displayed in Figure 6. For all samples, the majority of the LILs signals is attributed to β-O-4 aryl ether bonds while weak signals result from the C_α-H_α and C_β-H_β of phenylcoumaran linkages. This observation comforts the py-GC/MS hypothesis emitted on the basis of the lignin fragmentation pattern. In agreement with the global analyses, the anomeric carbon signals from hemicelluloses detected in the aliphatic region are attributed to mannose, glucose and galactose units. The two cross peak signals at δ_C/δ_H 71.3/5.28 and 73.9/4.85 ppm, which are omnipresent in the spectra, indicate that the hydroxyl groups on carbon 2 and 3 of mannose units are partially acetylated in all samples. This acetylation pattern is current in native hemicelluloses of softwood and its preservation throughout the extraction and downstream processes is an evidence of the mildness of the overall process.[32] Concerning the LCLs, only phenyl glycosidic bond signals are detected in the aliphatic region of all spectra. In general, no additional signals appeared in the spectra of the LCC rich fraction after the different DSP when compared with the freeze-dried sample. If occurring, alteration of the LCCs structure by the DSP would have led to the appearance of new signals such as Hibbert's ketones structures arising from aryl ether bond cleavage or mannose acetylated carbon 6 arising from trans-acetylation as described in the literature.[4,25]

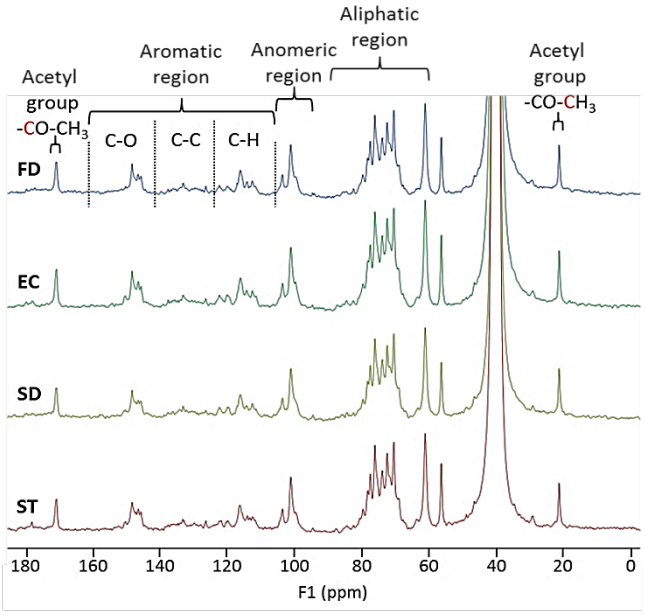

Figure 7. ^{13}C NMR spectra of the four samples with delimited signal regions: C-O: oxygenated carbons, C-C: condensed carbons and C-H: protonated carbons.

Quantitative ^{13}C NMR spectra of the four samples are shown in Figure 7. The identification of the different integrated regions is indicated. The exact delimitation and integral values are given in supporting information (Table S3). Information about the lignin condensation degree can be deduced from this analysis as previously reported.[17,33] The condensation degree is calculated as the ratio of the condensed aromatic integral value on the protonated aromatic one. For quantification of LILs and LCLs, the aromatic regions (105-160 ppm) of all spectra were integrated and normalised to 600 resulting that the integral values of the other regions were expressed per 100 aromatic rings. Those integrals were used to convert the relative signals elucidated by 2D-HSQC into ^{13}C based number per aromatic rings (n°/100ar) as previously reported in the literature.[4,6,17,34] Calculations were done using the following equations (1) and (2):

$$\frac{PhG}{100ar} = 600 * \frac{2D_{PhG}}{2D_{(105-94;5.5-4)}} * \frac{13C_{(105-94)}}{13C_{(160-105)}} \quad (1)$$

$$\frac{LIL}{100ar} = 600 * \frac{2D_{LIL}}{2D_{(90-80;6-2.5)}} * \frac{13C_{(90-80)}}{13C_{(160-105)}} \quad (2)$$

The acetylation patterns of the samples were semi-quantified on the basis of the 2D-HSQC signals and HPAEC sugar analysis results (Table 1) as described by Giummarella *et al.* The following equation (3) gives as an example the calculation of the mannose carbon 2 acetylation degree:

$$\mathrm{M_{C2\text{-}ac}\ (mol\%\ of\ Man)} = \frac{\mathrm{2D(M_{C2\text{-}ac})} \times 10^4}{\mathrm{M_{mol\%}(HPAEC)} \times \mathrm{2D(C_{1\ anomeric})}} \quad (3)$$

The acetylation degree of mannose carbon 2 ($M_{C2\text{-}ac}$) is expressed as molar % of total mannose units (mol% of Man). 2D($M_{C2\text{-}ac}$) stands for the HSQC integral value of the mannose acetylated carbon 2 signal and 2D($C_{1\ anomeric}$) is the HSQC integral value of the C1 anomeric signal cluster (Table S4). The molar % of mannose unit on total carbohydrates quantified by HPAEC analysis (Mmol%(HPAEC)) is used to correct the relative signals from HSQC.

Table 4. Quantification of the LILs, LCLs (n°/100ar) and acetylation pattern (mol% of Man) of the four samples.

	Previous data[17]	FD	EC	SD	ST
Hemicelluloses					
M_2-acetylation degree	-	23.3	23.2	22.3	22.0
M_3-acetylation degree	-	14.5	15.7	15.6	14.8
Lignin structure					
β-O-4' (A)	36.6	7.7	8.1	7.7	7.8
β-5' (B)	4.1	1.2	1.4	1.5	1.6
Condensation degree	0.66	0.70	0.54	0.66	0.60
LCCs linkages					
PhG	25.5	14.1	15.7	14.1	13.8

The quantification results are summarised in Table 4 and compared to previous published data on the freeze-dried fraction.[17] The condensation degree of the lignin moiety in LCCs remain perfectly stable at around 0.60 throughout all the DSP which means that no condensation reactions were triggered by the different processes. In other words, the carbon-carbon branching patter of the aromatic rings in LCCs did not evolve during the DSP. The acetylation pattern of the hemicellulosic moiety of LCC is also well preserved. Around 23 % of the carbons 2 in mannose units are acetylated and 15 % of the carbons 3. These quantifications are consistent with the data reported for native GGM in the literature where the M2-ac degree range from 20 to 36 % and the M3-ac is comprised between 16 to 19%.[4,32] Concerning the LILs and LCLs, the values found in this work are markedly smaller than the ones previously published for the freeze-dried sample. As the aim of the analysis was to generate comparative data (not absolute characterizations of the samples) a less performing NMR equipment was used in this study (300 MHz against 400 MHz previously). The lowest resolution of the spectra is probably responsible for the underestimation of the structures. A control set of data was generated for the freeze-dried and spray-dried samples using a 400 MHz NMR spectrometer to be sure that this signal loss did not lead to a distorted view of the spectra (Table S4). In both conditions (300 and 400 MHz), the different samples present really near LILs and LCLs contents between them as expected with the excellent stackability of the ^{13}C and 2D spectra. Even if the absolute values have to be taken with caution, this set of experiments demonstrates that the resolution of a 300 MHz spectrometer is enough to get representative NMR data for comparison studies. The conclusion for both conditions is that the thermally unstable ether bonds and functional groups were efficiently preserved during the DSP. The previous observations made by visual comparison are reinforced by the quantified data extracted from the different spectra.

Concluding discussion. The DSP applied in this work were optimized in order to minimize the heat exposure of LCCs as the poor thermal stability of lignin and hemicelluloses are of common knowledge. The maximum temperature used reached 190 °C during spray-drying while the working temperature of simple effect evaporation and moist heat sterilization were maintained between 85 and 121°C but the samples were kept under pressurized atmospheres. At similar temperatures, Giummarella *et al.* observed structural modifications of LCCs during hydrothermal treatment of softwood (160 °C, 2 h) including 25 % of diminution in the β-O-4 content.[4] The main structures cleaved during heat exposure are the labile ether and ester bonds. Such cleavages lead to the production of new oxidized end groups or trigger random polymerization (condensation) reactions and directly impact the functionalization, internal structure and molecular weight of the macromolecules.

All of these parameters were monitored by the combination of performant analytical tools to follow the evolution of the lignin rich fraction throughout the different DSP which could be used for its production at industrial scale and commercialization. Thermal fragmentation pattern, condensation degree and interunit linkage contents were used to evaluate the lignin moiety. Elemental analysis and NMR brought information on the functionalization of LCC and SEC on their aMW. Altogether, the results indicate that all the structures, hemicelluloses and lignin moieties, are perfectly well preserved during the processes, under the specified conditions. The short time heat exposure of LCCs during spray-drying is suitable to preserve their structure and the pressure applied during the other processes does not add up any negative effect such as favoring hemicelluloses autohydrolysis. The combination of simple effect evaporation and spray-drying allowed the production of a fine powder, easy to handle and store, while preserving the structure and properties of the LCCs recovered from the residual feedstock. This work proposes a complete and optimized process for LCCs production at an industrial level.

ASSOCIATED CONTENT

Peaks identification in Py-GC/MS, signals assignment in ^{13}C and 2D HSQC NMR, quantification results of 400 MHz NMR experiments as well as the aromatic region of the 2D HSQC spectra are available as Supporting Information Supplemental (PDF).

AUTHOR INFORMATION

Corresponding Author

* Corresponding author email: maud.villain@unistra.fr, tel: +33(0)368852748

Author Contributions

The manuscript was written through contributions of all authors. All authors have given approval to the final version of the manuscript.

Note

The authors declare no competing financial interest.

ACKNOWLEDGMENT

The NMR platform team form the Institut Jean Barriol, and in particular Mrs Sophie Poinsignon, is gratefully acknowledged for its technical support and contribution.

REFERENCES

(1) Lawoko, M.; Henriksson, G.; Gellerstedt, G. Characterisation of Lignin-Carbohydrate Complexes (LCCs) of Spruce Wood (Picea Abies L.) Isolated with Two Methods. *Holzforschung* **2006**, *60* (2), 156–161. https://doi.org/10.1515/HF.2006.025.

(2) Lawoko, M.; Henriksson, G.; Gellerstedt, G. New Method for Quantitative Preparation of Lignin- Carbohydrate Complex from Unbleached Softwood Kraft Pulp: Lignin-Polysaccharide Networks I. *Holzforschung* **2003**, *57* (1). https://doi.org/10.1515/HF.2003.011.

(3) Lawoko, M.; Berggren, R.; Berthold, F.; Henriksson, G.; Gellerstedt, G. Changes in the Lignin-Carbohydrate Complex in Softwood Kraft Pulp during Kraft and Oxygen Delignification. *Holzforschung* **2004**, *58* (6). https://doi.org/10.1515/HF.2004.114.

(4) Giummarella, N.; Lawoko, M. Structural Insights on Recalcitrance during Hydrothermal Hemicellulose Extraction from Wood. *ACS Sustain. Chem. Eng.* **2017**, *5* (6), 5156–5165. https://doi.org/10.1021/acssuschemeng.7b00511.
(5) You, T.-T.; Zhang, L.-M.; Zhou, S.-K.; Xu, F. Structural Elucidation of Lignin–Carbohydrate Complex (LCC) Preparations and Lignin from Arundo Donax Linn. *Ind. Crops Prod.* **2015**, *71*, 65–74. https://doi.org/10.1016/j.indcrop.2015.03.070.
(6) Narron, R. H.; Chang, H.; Jameel, H.; Park, S. Soluble Lignin Recovered from Biorefinery Pretreatment Hydrolyzate Characterized by Lignin–Carbohydrate Complexes. *ACS Sustain. Chem. Eng.* **2017**, *5* (11), 10763–10771. https://doi.org/10.1021/acssuschemeng.7b02716.
(7) Oinonen, P.; Krawczyk, H.; Ek, M.; Henriksson, G.; Moriana, R. Bioinspired Composites from Cross-Linked Galactoglucomannan and Microfibrillated Cellulose: Thermal, Mechanical and Oxygen Barrier Properties. *Carbohydr. Polym.* **2016**, *136*, 146–153. https://doi.org/10.1016/j.carbpol.2015.09.038.
(8) Uraki, Y.; Usukura, Y.; Kishimoto, T.; Ubukata, M. Amphiphilicity of a Lignin-Carbohydrate Complex. *Holzforschung* **2006**, *60* (6). https://doi.org/10.1515/HF.2006.111.
(9) Zhao, H.; Li, J.; Wang, P.; Zeng, S.; Xie, Y. Lignin-Carbohydrate Complexes Based Spherical Biocarriers: Preparation, Characterization, and Biocompatibility https://www.hindawi.com/journals/ijps/2017/4915185/ (accessed Nov 13, 2018). https://doi.org/10.1155/2017/4915185.
(10) Sakagami, H.; Sheng, H.; Okudaira, N.; Yasui, T.; Wakabayashi, H.; Jia, J.; Natori, T.; Suguro-Kitajima, M.; Oizumi, H.; Oizumi, T. Prominent Anti-UV Activity and Possible Cosmetic Potential of Lignin-Carbohydrate Complex. *In Vivo* **2016**, *30* (4), 331–339.
(11) Zhang, Y.; Wang, S.; Xu, W.; Cheng, F.; Pranovich, A.; Smeds, A.; Willför, S.; Xu, C. Valorization of Lignin–Carbohydrate Complexes from Hydrolysates of Norway Spruce: Efficient Separation, Structural Characterization, and Antioxidant Activity. *ACS Sustain. Chem. Eng.* **2019**, *7* (1), 1447–1456. https://doi.org/10.1021/acssuschemeng.8b05142.
(12) Zhang, Y.; But, P. P.-H.; Ooi, V. E.-C.; Xu, H.-X.; Delaney, G. D.; Lee, S. H. S.; Lee, S. F. Chemical Properties, Mode of Action, and in Vivo Anti-Herpes Activities of a Lignin–Carbohydrate Complex from Prunella Vulgaris. *Antiviral Res.* **2007**, *75* (3), 242–249. https://doi.org/10.1016/j.antiviral.2007.03.010.
(13) Huang, C.; Tang, S.; Zhang, W.; Tao, Y.; Lai, C.; Li, X.; Yong, Q. Unveiling the Structural Properties of Lignin–Carbohydrate Complexes in Bamboo Residues and Its Functionality as Antioxidants and Immunostimulants. *ACS Sustain. Chem. Eng.* **2018**, *6* (9), 12522–12531. https://doi.org/10.1021/acssuschemeng.8b03262.
(14) Du, X.; Gellerstedt, G.; Li, J. Universal Fractionation of Lignin-Carbohydrate Complexes (LCCs) from Lignocellulosic Biomass: An Example Using Spruce Wood. *Plant J.* **2013**, *74* (2), 328–338. https://doi.org/10.1111/tpj.12124.
(15) Westerberg, N.; Sunner, H.; Helander, M.; Henriksson, G.; Lawoko, M.; Rasmuson, A. Separation of galactoglucomannans, lignin, and lignin-carbohydrate complexes from hot-water-extracted norway spruce by cross-flow filtration and adsorption chromatography. *BioResources* **2012**, *7* (4), 4501–4516. https://doi.org/10.15376/biores.7.4.4501-4516.
(16) Al-Rudainy, B.; Galbe, M.; Wallberg, O. Influence of Prefiltration on Membrane Performance during Isolation of Lignin-Carbohydrate Complexes from Spent Sulfite Liquor. *Sep. Purif. Technol.* **2017**, *187*, 380–388. https://doi.org/10.1016/j.seppur.2017.06.031.

(17) Steinmetz, V.; Villain-Gambier, M.; Klem, A.; Gambier, F.; Dumarcay, S.; Trebouet, D. Unveiling TMP Process Water Potential As an Industrial Sourcing of Valuable Lignin–Carbohydrate Complexes toward Zero-Waste Biorefineries. *ACS Sustain. Chem. Eng.* **2019**, *7* (6), 6390–6400. https://doi.org/10.1021/acssuschemeng.9b00181.
(18) Lei, Z.; Wang, S.; Fu, H.; Gao, W.; Wang, B.; Zeng, J.; Xu, J. Thermal Pyrolysis Characteristics and Kinetics of Hemicellulose Isolated from Camellia Oleifera Shell. *Bioresour. Technol.* **2019**, *282*, 228–235. https://doi.org/10.1016/j.biortech.2019.02.131.
(19) Kim, J.-Y.; Hwang, H.; Oh, S.; Kim, Y.-S.; Kim, U.-J.; Choi, J. W. Investigation of Structural Modification and Thermal Characteristics of Lignin after Heat Treatment. *Int. J. Biol. Macromol.* **2014**, *66*, 57–65. https://doi.org/10.1016/j.ijbiomac.2014.02.013.
(20) Rousset, P.; Lapierre, C.; Pollet, B.; Quirino, W.; Perre, P. Effect of Severe Thermal Treatment on Spruce and Beech Wood Lignins. *Ann. For. Sci.* **2009**, *66* (1), 110–110. https://doi.org/10.1051/forest/2008078.
(21) Wang, S.; Ru, B.; Lin, H.; Sun, W.; Luo, Z. Pyrolysis Behaviors of Four Lignin Polymers Isolated from the Same Pine Wood. *Bioresour. Technol.* **2015**, *182*, 120–127. https://doi.org/10.1016/j.biortech.2015.01.127.
(22) Li, H.; McDonald, A. G. Fractionation and Characterization of Industrial Lignins. *Ind. Crops Prod.* **2014**, *62*, 67–76. https://doi.org/10.1016/j.indcrop.2014.08.013.
(23) Shishir, M. R. I.; Chen, W. Trends of Spray Drying: A Critical Review on Drying of Fruit and Vegetable Juices. *Trends Food Sci. Technol.* **2017**, *65*, 49–67. https://doi.org/10.1016/j.tifs.2017.05.006.
(24) Maltesen, M. J.; van de Weert, M. Drying Methods for Protein Pharmaceuticals. *Drug Discov. Today Technol.* **2008**, *5* (2–3), e81–e88. https://doi.org/10.1016/j.ddtec.2008.11.001.
(25) Constant, S.; Wienk, H. L. J.; Frissen, A. E.; Peinder, P. de; Boelens, R.; van Es, D. S.; Grisel, R. J. H.; Weckhuysen, B. M.; Huijgen, W. J. J.; Gosselink, R. J. A.; et al. New Insights into the Structure and Composition of Technical Lignins: A Comparative Characterisation Study. *Green Chem.* **2016**, *18* (9), 2651–2665. https://doi.org/10.1039/C5GC03043A.
(26) Werner, K.; Pommer, L.; Broström, M. Thermal Decomposition of Hemicelluloses. *J. Anal. Appl. Pyrolysis* **2014**, *110*, 130–137. https://doi.org/10.1016/j.jaap.2014.08.013.
(27) del Río, J. C.; Speranza, M.; Gutiérrez, A.; Martínez, M. J.; Martínez, A. T. Lignin Attack during Eucalypt Wood Decay by Selected Basidiomycetes: A Py-GC/MS Study. *J. Anal. Appl. Pyrolysis* **2002**, *64* (2), 421–431. https://doi.org/10.1016/S0165-2370(02)00043-8.
(28) del Río, J. C.; Gutiérrez, A.; Martínez, M. J.; Martínez, A. T. Py–GC/MS Study of Eucalyptus Globulus Wood Treated with Different Fungi. *J. Anal. Appl. Pyrolysis* **2001**, *58–59*, 441–452. https://doi.org/10.1016/S0165-2370(00)00184-4.
(29) Giummarella, N.; Zhang, L.; Henriksson, G.; Lawoko, M. Structural Features of Mildly Fractionated Lignin Carbohydrate Complexes (LCC) from Spruce. *RSC Adv.* **2016**, *6* (48), 42120–42131. https://doi.org/10.1039/C6RA02399A.
(30) Balakshin, M.; Capanema, E.; Gracz, H.; Chang, H.; Jameel, H. Quantification of Lignin–Carbohydrate Linkages with High-Resolution NMR Spectroscopy. *Planta* **2011**, *233* (6), 1097–1110. https://doi.org/10.1007/s00425-011-1359-2.
(31) González Martínez, M.; Ohra-aho, T.; Tamminen, T.; da Silva Perez, D.; Campargue, M.; Dupont, C. Detailed Structural Elucidation of Different Lignocellulosic Biomass Types Using Optimized Temperature and Time Profiles in Fractionated Py-GC/MS. *J. Anal. Appl. Pyrolysis* **2019**, *140*, 112–124. https://doi.org/10.1016/j.jaap.2019.02.011.

(32) Willför, S.; Sjöholm, R.; Laine, C.; Roslund, M.; Hemming, J.; Holmbom, B. Characterisation of Water-Soluble Galactoglucomannans from Norway Spruce Wood and Thermomechanical Pulp. *Carbohydr. Polym.* **2003**, *52* (2), 175–187. https://doi.org/10.1016/S0144-8617(02)00288-6.
(33) Brosse, N.; El Hage, R.; Chaouch, M.; Pétrissans, M.; Dumarçay, S.; Gérardin, P. Investigation of the Chemical Modifications of Beech Wood Lignin during Heat Treatment. *Polym. Degrad. Stab.* **2010**, *95* (9), 1721–1726. https://doi.org/10.1016/j.polymdegradstab.2010.05.018.
(34) Yuan, T.-Q.; Sun, S.-N.; Xu, F.; Sun, R.-C. Characterization of Lignin Structures and Lignin–Carbohydrate Complex (LCC) Linkages by Quantitative 13C and 2D HSQC NMR Spectroscopy. *J. Agric. Food Chem.* **2011**, *59* (19), 10604–10614. https://doi.org/10.1021/jf2031549.

TABLE OF CONTENTS GRAPHIC

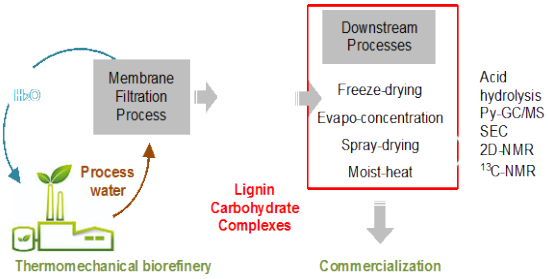

SYNOPSIS

This work proposes a sustainable and optimized industrial process for integrated biorefineries targeting LCCs commercialization after recovery from their residual feedstocks.